

# Estrogen Treatment After Ovariectomy Protects Against Fatty Liver and May Improve Pathway-Selective Insulin Resistance

Lin Zhu,<sup>1</sup> William C. Brown,<sup>1,2</sup> Qing Cai,<sup>3</sup> Andrée Krust,<sup>4</sup> Pierre Chambon,<sup>4</sup> Owen P. McGuinness,<sup>3</sup> and John M. Stafford<sup>1,3,5</sup>

Pathway-selective insulin resistance where insulin fails to suppress hepatic glucose production but promotes liver fat storage may underlie glucose and lipid abnormalities after menopause. We tested the mechanisms by which estrogen treatment may alter the impact of a high-fat diet (HFD) when given at the time of ovariectomy (OVX) in mice. Female C57BL/6J mice underwent sham operation, OVX, or OVX with estradiol (E2) treatment and were fed an HFD. Hyperinsulinemic-euglycemic clamps were used to assess insulin sensitivity, tracer incorporation into hepatic lipids, and liver triglyceride export. OVX mice had increased adiposity that was prevented with E2 at the time of OVX. E2 treatment increased insulin sensitivity with OVX and HFD. In sham and OVX mice, HFD feeding induced fatty liver, and insulin reduced hepatic apoB100 and liver triglyceride export. E2 treatment reduced liver lipid deposition and prevented the decrease in liver triglyceride export during hyperinsulinemia. In mice lacking the liver estrogen receptor  $\alpha$ , E2 after OVX limited adiposity but failed to improve insulin sensitivity, to limit liver lipid deposition, and to prevent insulin suppression of liver triglyceride export. In conclusion, estrogen treatment may reverse aspects of pathway-selective insulin resistance by promoting insulin action on glucose metabolism but limiting hepatic lipid deposition. *Diabetes* 62:424–434, 2013

**W**ith overnutrition, insulin resistance impairs insulin's ability to suppress gluconeogenesis resulting in fasting hyperglycemia (1,2). By contrast, insulin robustly promotes liver fatty acid synthesis and decreases fatty acid oxidation (3–6). In fasting, this fatty liver increases triglyceride secretion in the form of VLDL and subsequently leads to decreased HDL (3,4,6–8). Insulin signaling also promotes degradation of apolipoprotein (apo)B100 in the liver, thus limiting secretion of VLDL from the liver (9). In these studies, we define how estrogen treatment may modulate pathway-selective insulin resistance and the development of fatty liver with high-fat diet (HFD) feeding in mice.

From the <sup>1</sup>Tennessee Valley Healthcare System, Nashville, Tennessee; the <sup>2</sup>Division of Diabetes, Endocrinology, and Metabolism, Department of Internal Medicine, Vanderbilt University School of Medicine, Nashville, Tennessee; the <sup>3</sup>Department of Molecular Physiology and Biophysics, Vanderbilt University School of Medicine, Nashville, Tennessee; <sup>4</sup>Institut de Génétique et de Biologie Moléculaire et Cellulaire, Illkirch, France; and <sup>5</sup>Case Western Reserve Medical Center, Cleveland, Ohio.

Corresponding author: John M. Stafford, john.stafford@vanderbilt.edu.

Received 9 December 2011 and accepted 6 August 2012.

DOI: 10.2337/db11-1718

This article contains Supplementary Data online at <http://diabetes.diabetesjournals.org/lookup/suppl/doi:10.2337/db11-1718/-/DC1>.

© 2013 by the American Diabetes Association. Readers may use this article as long as the work is properly cited, the use is educational and not for profit, and the work is not altered. See <http://creativecommons.org/licenses/by-nc-nd/3.0/> for details.

Premenopausal women are protected from the cardiovascular complications of obesity compared with BMI-matched men. This protection may relate to estrogen's ability to limit liver fat accumulation, thus preventing hepatic insulin resistance (10,11). The triglyceride content of VLDL in women is increased by ~70% compared with men without a difference in VLDL particle number (12–14). In insects, birds, and fish, estrogen-like pathways increase transport of triglyceride from the liver to facilitate egg development (15). Estrogen also promotes fatty acid oxidation in the liver. During menopause, liver lipids accumulate in the liver. We propose that estrogen treatment might promote fatty acid oxidation and increase the efficiency triglyceride export out of the liver, which might limit liver fat and improve glucose metabolism with HFD feeding.

In these studies, we define the mechanisms by which estrogen treatment at the time of surgical menopause (ovariectomy [OVX]) might improve the regulation of glucose and triglyceride metabolism. The metabolic effects of estrogen with regard to body weight regulation and fat storage are largely mediated by estrogen receptor  $\alpha$  (ER $\alpha$ ) (16,17). Mice with global ER $\alpha$  deletion have increased adiposity and insulin resistance (11,18,19). ER $\alpha$  signaling is also involved in LDL and HDL kinetics (20), protecting against the  $\beta$ -cell dysfunction that can accompany obesity (21) and integrating nutritional signaling (16). The role of liver ER $\alpha$  with regard to hepatic glucose and lipid metabolism is not well defined. We found that estrogen treatment reduces insulin-mediated liver fat storage and reduces diacylglycerol content and yet promotes insulin action with regard to glucose metabolism. This protective effect of estrogen treatment requires intact hepatic estrogen signaling through ER $\alpha$ . By contrast, we found that hepatic estrogen signaling is not required for the effects of estrogen treatment on body weight and adiposity.

## RESEARCH DESIGN AND METHODS

Seven-week-old female C57BL/6J mice (17–19 g, strain 000664; The Jackson Laboratory, Bar Harbor, ME) were housed at 22  $\pm$  1°C in a 12:12-h light:dark cycle. Mice with liver-specific deletion of ER $\alpha$  on a C57BL/6J background (LKO) were made by breeding ER $\alpha$  flox/flox mice with mice expressing cre recombinase under the control of the albumin promoter (The Jackson Laboratory) (16,22,23). Protocols were approved by the institutional animal care and use committee at Vanderbilt University.

**Experimental design.** Mice were matched for body composition ( $n = 6$ –10 per group) and underwent sham operation, bilateral OVX, or OVX with a subcutaneous implantation of 17 $\beta$ -estradiol sustained release tablet at the time of OVX (0.25 mg/pellet, 60-day release; Innovative Research of America, Sarasota, FL). All mice were maintained on an HFD (cat. no. D08060104, 60% fat from lard, 20% protein, 20% carbohydrate from corn starch, 5.24 kcal/g; Research Diets).

**Surgical catheterization.** After 5 weeks of HFD feeding, catheters were implanted by the Vanderbilt Mouse Metabolic Phenotyping Center in the left

common carotid artery and right jugular vein for sampling and infusions as previously described (24).

**Hyperinsulinemic-euglycemic clamps.** Five to seven days after catheter placement, hyperinsulinemic-euglycemic clamps were performed in unrestrained 5-h-fasted mice. A primed (4.80  $\mu\text{Ci}$ ) continuous (0.1067  $\mu\text{Ci}/\text{min}$ ) infusion of U- $^{14}\text{C}$ -glycerol was initiated at  $t = -180$  min (9:00 A.M.) and continued for the duration of the study. A primed (5.4  $\mu\text{Ci}$ ) continuous (0.135  $\mu\text{Ci}/\text{min}$ ) infusion of 3- $^3\text{H}$ -glucose was initiated at  $t = -90$  min. The period between  $t = -180$  and  $t = 0$  allowed us to assess basal tracer incorporation into VLDL and glucose production. This basal period was followed by hyperinsulinemia started at  $t = 0$  (4 mU/kg/min; Humulin R; Eli Lilly, Indianapolis, IN). At  $t = 0$  min, the infusion rate was increased to 0.27  $\mu\text{Ci}/\text{min}$ . Euglycemia ( $\sim 150$  mg/dL) was maintained by measuring blood glucose every 10 min starting at  $t = 0$  min and adjusting the infusion of 50% dextrose as necessary. Mice received saline-washed erythrocytes from donors to prevent a fall in hematocrit. At  $t = 120$  min, mice were killed and tissues were flash frozen. To obtain non-insulin-treated samples, a parallel set of experiments was performed in which mice were fed an HFD for 6 weeks, fasted 5 h, and then killed.

**Plasma processing and calculations.** Insulin levels were determined by ELISA (cat. no. EZRMI-13K; Millipore, St. Charles, MO). Plasma  $^{14}\text{C}$ -triglyceride activities were divided by plasma triglyceride to define triglyceride-specific activity. In the fasting state, the triglyceride-specific activity is an index of VLDL flux. 3- $^3\text{H}$ -glucose activities were determined by liquid scintillation counting after plasma deproteinization. Glucose  $R_d$  and endogenous glucose production (EndoRa) were determined using non-steady state equations, and insulin sensitivity index was calculated as previously described (24–26).

**Liver triglyceride content analysis.** Liver neutral lipids were stained with oil red O. Liver lipid was extracted using Folch methodology, and triglyceride and diacylglycerol were separated by thin-layer chromatography (TLC) as previously described (27). Total liver triglyceride amount was quantified using triglycerides GPO reagents according to the manufacturer's protocol (Cliniqa); diacylglycerol amounts were evaluated using the same reagents and protocols by adjusting the standard value of glycerol.  $^{14}\text{C}$ -triglyceride and  $^{14}\text{C}$ -diacylglycerol were determined by scintillation counting after TLC separation and normalized to tissue weight.

**Protein immunoblots.** Western blots were performed as previously described (28). Antibodies for AMP kinase (AMPK) $\alpha$  (cat. no. 2603), phosphorylated AMPK $\alpha$  ( $^{172}\text{Thr}$ , cat. no. 2535), AMPK $\beta$  (cat. no. 4150), and phospho-AMPK $\beta$  ( $^{108}\text{Ser}$ , cat. no. 4181) were from Cell Signaling (Beverly, MA); antibodies for diacylglycerol acyltransferase (DGAT)1 (sc-31680), DGAT2 (sc-66859), and  $\beta$ -actin (sc-47778) were from Santa Cruz Biotech (Santa Cruz, CA); antibody for ApoB100 was from LifeSpan BioSciences (LS-c20729). Anti-MTP antibody was provided by Dr. Larry Swift (29). Anti-mouse or anti-rabbit antibody was incubated with the dilution of 1:15,000 at room temperature for 1 h. Imaging and densitometry were performed using the Odyssey imaging system (LI-COR Biosciences, Lincoln, NE) and ImageJ processing program.

**Statistical analysis.** Data are presented as means  $\pm$  SD. Differences between groups were determined by ANOVA followed by Tukey post hoc tests or by Student  $t$  test as appropriate. Significance was considered as  $P < 0.05$ .

## RESULTS

**Estrogen treatment at the time of OVX improves diet-induced obesity and insulin sensitivity.** For definition of the effects of estrogen treatment on obesity, dyslipidemia, and glucose metabolism, sham, OVX, or OVX+E2 mice were put on an HFD for a total of 6 weeks. We found that sham mice had a 32% increase in body weight and a 46% increase in adiposity (Fig. 1A and B) ( $P < 0.05$  for both compared with baseline) and OVX mice had a 77% increase in body weight and 278% increase in adiposity after HFD feeding (Fig. 1A and B) ( $P < 0.05$  for both). By contrast, estrogen-treated mice did not gain weight or have increased adiposity with OVX and HFD feeding (Fig. 1A and B). Thus, the absence of ovarian hormones predisposes to weight gain on HFD, and estrogen treatment was associated with reduced adiposity with OVX and HFD.

We evaluated the impact of OVX and estrogen treatment on serum lipids. Loss of ovarian hormones by OVX increased the fasting plasma cholesterol concentration compared with sham mice, which was prevented with estrogen treatment (Fig. 1C). Serum triglyceride levels were elevated with HFD feeding in sham mice compared

with a group of chow-fed female controls ( $45 \pm 7$  mg/dL [not shown on the figure]); OVX did not further increase fasting serum triglyceride compared with HFD-fed sham mice. Mice with estrogen treatment did not have elevated serum triglyceride after OVX and HFD, and triglyceride levels were similar to those of chow-fed female controls (Fig. 1D) ( $45 \pm 7$  mg/dL for chow-fed female controls).

To obtain an index of what estrogen treatment did to insulin sensitivity, we examined fasting glucose and insulin levels. In sham mice with HFD feeding, fasting insulin levels were increased approximately threefold compared with chow-fed female controls (Fig. 1E) ( $10 \pm 2$   $\mu\text{U}/\text{mL}$  for chow-fed controls [not shown in Fig. 1]). Fasting insulin levels were further increased in OVX mice. By contrast, estrogen treatment was associated with lower fasting insulin (Fig. 1E). There were no differences in fasting glucose levels between groups (Fig. 1F). These findings demonstrate that estrogen treatment was associated with a reduction in fasting insulin proportional to adiposity.

**Insulin regulation of hepatic and peripheral glucose metabolism is maintained with HFD feeding with estrogen treatment after OVX.** We designed a study to assess baseline hepatic glucose and triglyceride secretion and then initiated a hyperinsulinemic-euglycemic clamp to assess both insulin sensitivity and insulin's ability to suppress hepatic glucose production and triglyceride secretion (Fig. 2A). Blood glucose was matched between groups (Fig. 2B). The glucose infusion rate (GIR) required to maintain euglycemia is proportional to insulin sensitivity. We observed the lowest GIR in OVX mice and the highest GIR in OVX+E2 mice, and the GIR for sham mice was significantly higher than that for OVX (Fig. 2C). We also defined an insulin sensitivity index between groups by normalizing GIR to the plasma insulin concentration during the clamp period. Plasma insulin levels during the clamp were as follows: sham  $68 \pm 2$   $\mu\text{U}/\text{mL}$ , OVX  $84 \pm 20$   $\mu\text{U}/\text{mL}$ , and OVX+E2  $47 \pm 10$   $\mu\text{U}/\text{mL}$ . The insulin sensitivity index was significantly higher in OVX+E2 mice than in the other two groups (Fig. 2D). These data demonstrate that estrogen treatment improves insulin sensitivity after OVX and HFD.

We assessed whole-body and liver glucose metabolism during the clamp using a 3- $^3\text{H}$ -glucose tracer. Basal EndoRa was suppressed by hyperinsulinemia during the clamp in sham mice (Fig. 2E). By contrast, insulin-mediated suppression of EndoRa was impaired after OVX (Fig. 2E). Estrogen treatment was associated with improved ability of insulin to suppress EndoRa after OVX and HFD (Fig. 2E). Glucose  $R_d$  during the clamp was significantly higher with estrogen treatment in comparison with sham and OVX mice (Supplementary Fig. 1A). Thus, estrogen treatment improves hepatic and peripheral insulin action with regard to glucose metabolism after OVX.

**Estrogen treatment does not augment insulin-dependent suppression of tracer incorporation into serum triglyceride.** To evaluate the impact of estrogen treatment on insulin regulation of liver triglyceride production, we monitored plasma triglyceride and  $^{14}\text{C}$ -triglyceride-specific activity during fasting and hyperinsulinemic clamps. In all three groups, plasma triglyceride gradually decreased with the duration of fasting and did not decrease further during hyperinsulinemic clamps (Fig. 2F). For all groups of mice, plasma  $^{14}\text{C}$ -triglyceride-specific activity leveled off between  $t = -30$  and  $t = 0$  min (Fig. 2F). In OVX mice, this plateau was maintained

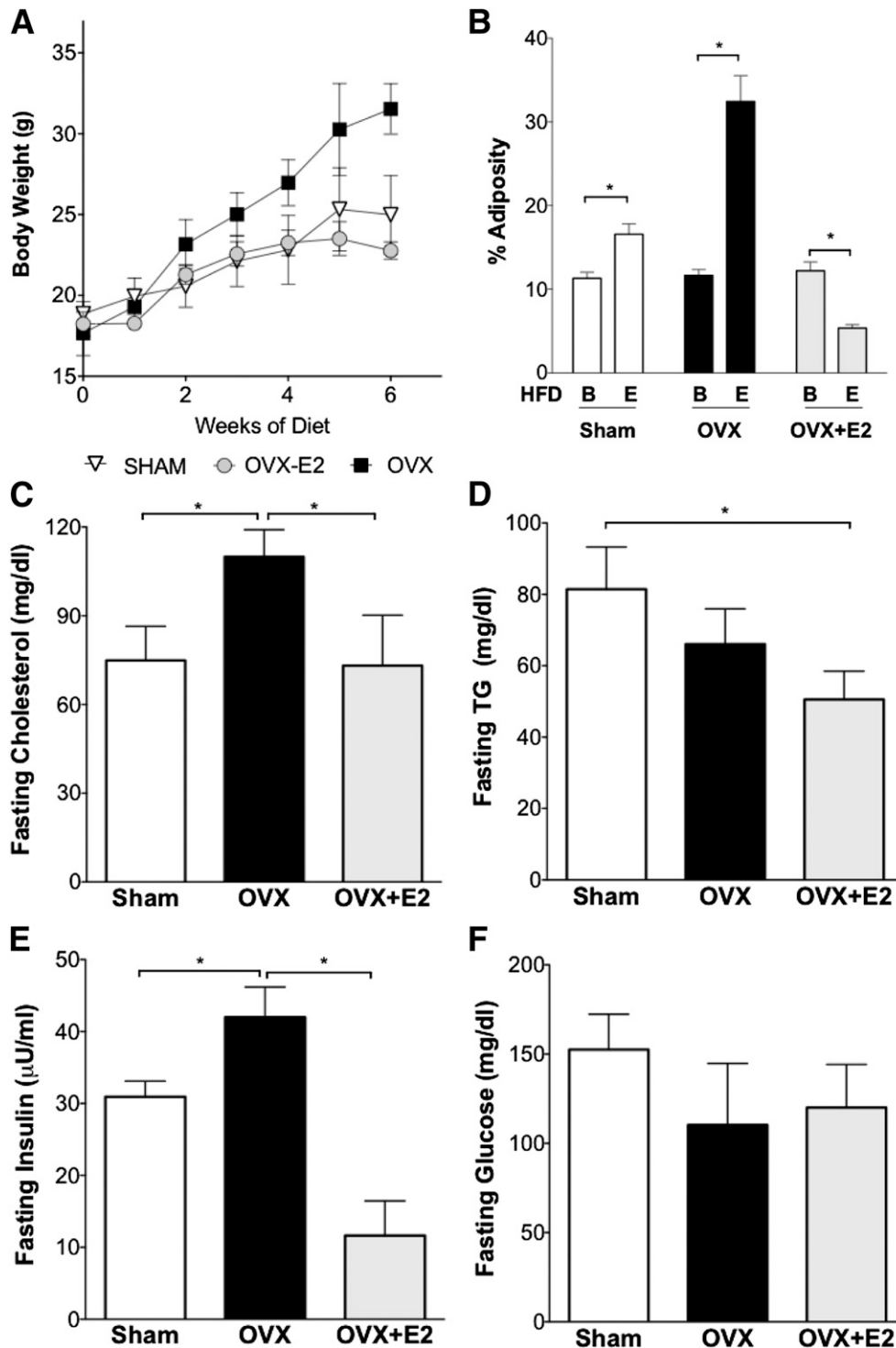


**FIG. 1.** Estrogen treatment at the time of OVX reduces diet-induced obesity. **A:** OVX led to increased body weight with HFD. Mice treated with E2 at the time of OVX did not gain weight with HFD. **B:** Adiposity was increased with HFD in sham mice and after OVX. Adiposity was reduced with E2 treatment. Letter B indicates baseline before HFD-feeding. Letter E indicates end point after HFD. **C:** Plasma cholesterol levels. **D:** Plasma triglyceride levels. **E:** HFD increased fasting insulin levels in sham and OVX mice, and E2 treatment reduced plasma insulin. **F:** Fasting glucose levels were not different between groups. \* $P < 0.05$ . For panel B, differences from baseline were defined by Student *t* test. For C–F, differences between groups were determined by ANOVA followed by Tukey post hoc tests.

during hyperinsulinemia. However, in OVX+E2 mice,  $^{14}$ C-triglyceride-specific activity failed to plateau during the hyperinsulinemic period. Sham mice had an intermediate phenotype (Fig. 2G). Together, these data suggest that estrogen treatment limits the ability of hyperinsulinemia to restrain the efficiency of liver

$^{14}$ C-triglyceride secretion, an index of VLDL secretion in these fasted mice.

The estrogen-dependent maintenance of tracer incorporation into serum triglyceride during hyperinsulinemia should then limit the deposition of lipid in the liver.

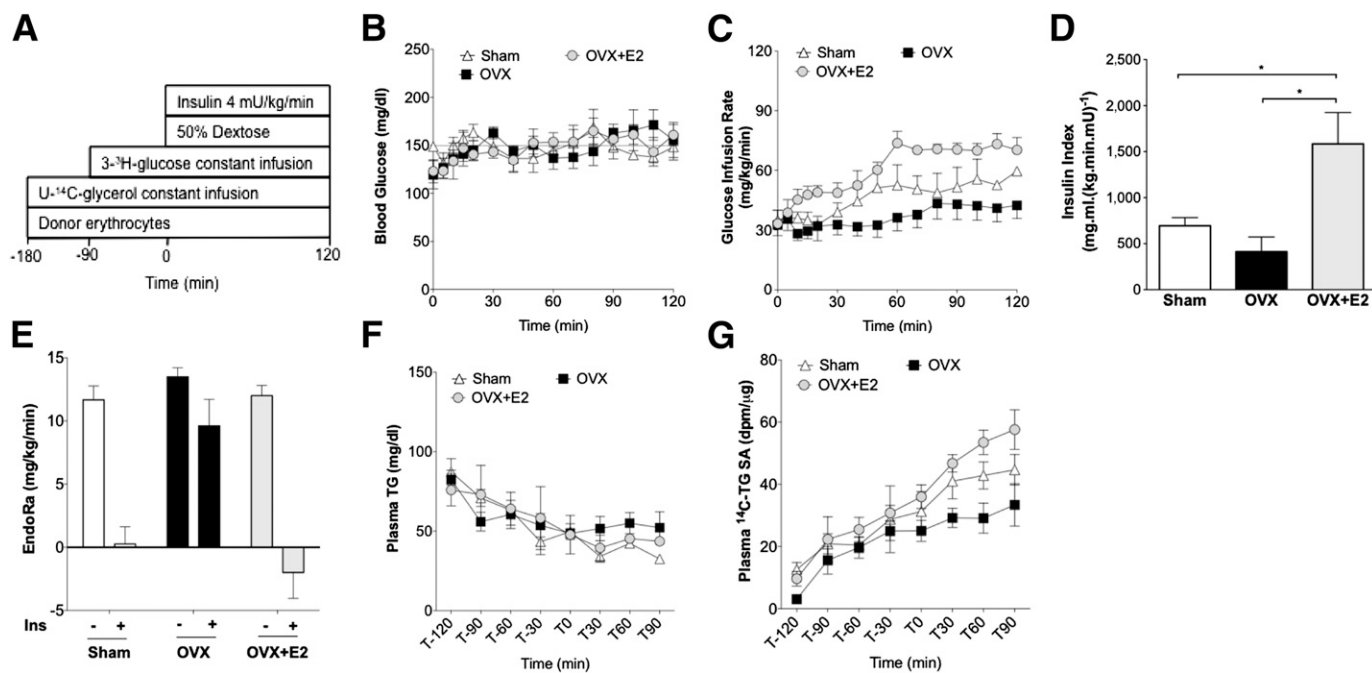


**FIG. 2.** Estrogen treatment at the time of OVX reduces pathway-selective insulin resistance. **A:** Schematic of the hyperinsulinemic-euglycemic clamp study with triglyceride (TG) and glucose tracers. **B:** Euglycemia was maintained at ~150 mg/dL during the clamp. **C:** GIR to maintain euglycemia. **D:** Insulin sensitivity index. **E:** Compared with baseline (no insulin), insulin failed to suppress EndoRa after OVX (plus insulin), but insulin did suppress EndoRa after OVX with E2 treatment. **F:** Total plasma triglyceride during the clamp study. **G:** Plasma  $^{14}\text{C}$ -triglyceride-specific activity (SA). \* $P < 0.05$ . Differences between groups were determined by ANOVA followed by Tukey post hoc tests.

### Estrogen treatment improves fatty liver and reduces liver diacylglycerol deposition during hyperinsulinemia.

Fatty liver and the accumulation of diacylglycerol may promote the development of hepatic insulin resistance (30). HFD feeding increased liver triglyceride 2.1-fold in sham mice (Fig. 3A and B) ( $17.0 \pm 3.8 \mu\text{g}/\text{mg}$ ) compared with chow-fed female controls ( $8.0 \pm 2.1 \mu\text{g}/\text{mg}$  [not shown in Fig. 3]). Liver triglyceride accumulation was more pronounced in OVX mice ( $24.7 \pm 5.2 \mu\text{g}/\text{mg}$ ). Estrogen treatment was associated with lower liver triglyceride with HFD and OVX (OVX+E2  $8.4 \pm 3.1 \mu\text{g}/\text{mg}$ ). In OVX mice, in parallel with increased liver triglyceride content, HFD feeding significantly increased liver total diacylglycerol levels (Fig. 3D). The liver diacylglycerol content in sham mice fed with HFD was 2.7-fold higher than in chow-fed female C57 mice (HFD  $0.62 \mu\text{g}/\text{mg}$  vs. chow  $0.23 \mu\text{g}/\text{mg}$ ,  $P < 0.05$ ). Liver diacylglycerol content was not further increased by OVX but was lower in estrogen-treated mice after OVX (Fig. 3D).

We determined liver triglyceride and diacylglycerol deposition by measuring the incorporation of  $^{14}\text{C}$ -glycerol into liver triglyceride (Fig. 3C) after the hyperinsulinemic clamps. The liver  $^{14}\text{C}$ -triglyceride in OVX mice was 1.4-fold higher than in sham mice. Triglyceride deposition was lower in estrogen-treated mice (65% less than OVX and 49% less than sham mice,  $P < 0.05$  for both). Similar to triglyceride deposition, estrogen was associated with lower diacylglycerol deposition after OVX (indicated by  $^{14}\text{C}$ -diacylglycerol) (Fig. 3E). These results suggest that estrogen treatment reduced liver triglyceride and diacylglycerol deposition associated with OVX and HFD. Liver levels of DGAT1/2 did not change between groups during either fasting or hyperinsulinemia (Supplementary Fig. 2). The reduced liver triglyceride and liver triglyceride deposition in OVX+E2 mice (Fig. 3) is consistent with the

maintenance of tracer incorporation into serum triglyceride during hyperinsulinemia (Fig. 2G).

**Estrogen treatment blocks insulin signaling to liver acetyl-CoA carboxylase.** Acetyl-CoA carboxylase (ACC) catalyzes the first step of fatty acid synthesis. Liver-specific deletion of ACC reduces hepatic triglyceride accumulation (31). We found that baseline ACC levels were elevated in OVX mice compared with sham and OVX+E2 mice (Fig. 4A and B). Increased ACC along with  $^{14}\text{C}$ -triglyceride levels (Fig. 4) suggests a contribution of triglyceride synthesis to liver fat deposition in mice without ovarian hormones. Phosphorylation of ACC (pACC) is an index of increased fatty acid oxidation and decreased fatty acid synthesis. We found increased pACC in non-insulin treated mice after OVX (Fig. 4A and C), consistent with other studies showing increased fatty acid oxidation associated with triglyceride accumulation in the liver (32,33).

After 2 h of hyperinsulinemia, pACC was decreased in sham mice. This decrease was less evident in mice after OVX, indicated by percent suppression by insulin (Fig. 4C). By contrast, pACC was increased in OVX+E2 mice despite hyperinsulinemia in the clamp study. This result suggests that estrogen treatment may decrease fatty acid synthesis and maintain fatty acid oxidation in the setting of hyperinsulinemia. In muscle, estrogen is known to activate AMPK and promote fatty acid oxidation (34). Our results do not appear to be mediated by AMPK, which was unchanged between groups (Supplementary Fig. 3).

**Estrogen treatment blocks the effects of hyperinsulinemia to reduce hepatic apoB100 and phospholipid transfer protein.** To define the mechanisms for maintained tracer incorporation into serum triglyceride during hyperinsulinemia in OVX+E2 mice, we compared levels of hepatic proteins involved in the regulation of VLDL secretion. During fasting, liver apoB100

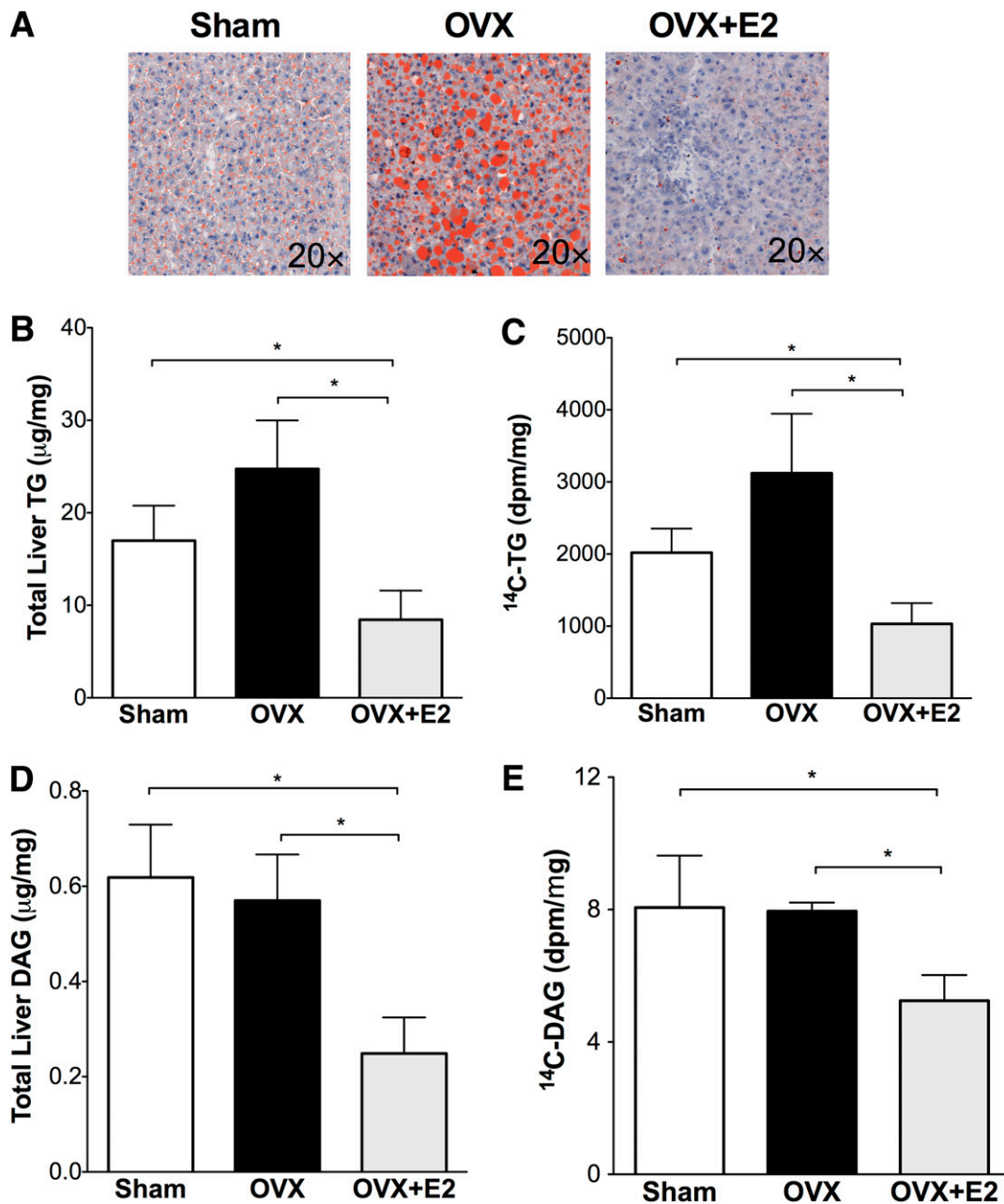


**FIG. 3.** Estrogen treatment at the time of OVX reduces fatty liver. *A*: Oil red O staining of liver neural lipid droplets. *B–E*: Liver lipids were extracted with the Folch method, and neutral lipids were separated by TLC as described in RESEARCH DESIGN AND METHODS. Triglyceride (TG) (*B*) and diacylglycerol (DAG) (*D*) were quantified using an enzymatic assay; <sup>14</sup>C-triglyceride (*C*) and <sup>14</sup>C-diacylglycerol (*E*) were quantified by scintillation counting. \**P* < 0.05. Differences between groups were determined by ANOVA followed by Tukey post hoc tests. (A high-quality digital representation of this figure is available in the online issue.)

protein levels were similar in sham, OVX, and OVX+E2 mice (Fig. 4*D* and *E*). Insulin decreased apoB100 for both sham and OVX mice (Fig. 4*D* and *E*). We found that insulin failed to decrease hepatic apoB100 in OVX+E2 mice, which was consistent with the accompanying maintenance of tracer incorporation into serum triglyceride during hyperinsulinemia (Fig. 2*G*). ApoB100 secretion is controlled in part by lipidation in endoplasmic reticulum by microsomal triglyceride transfer protein (MTP). We found that MTP levels were not changed between baseline and hyperinsulinemia or between groups (Fig. 4*D* and *F*). Phospholipid transfer protein (PLTP) promotes VLDL secretion by transferring phospholipids onto VLDL particles

(35). PLTP protein levels were reduced during hyperinsulinemia in sham and OVX mice. Insulin-mediated decrease in PLTP was prevented by estrogen treatment in mice (Fig. 4*D* and *G*). The results with PLTP are qualitatively similar to the liver apoB100 levels in these groups. This suggests that estrogen may promote lipid loading of apoB100 to maintain VLDL secretion in the setting of hyperinsulinemia, which would limit hepatic lipid deposition.

**Hepatic ER $\alpha$  signaling is required for estrogen to improve pathway-selective insulin resistance associated with HFD.** We used female mice with liver-specific knockout (LKO) of ER $\alpha$  to define the contribution

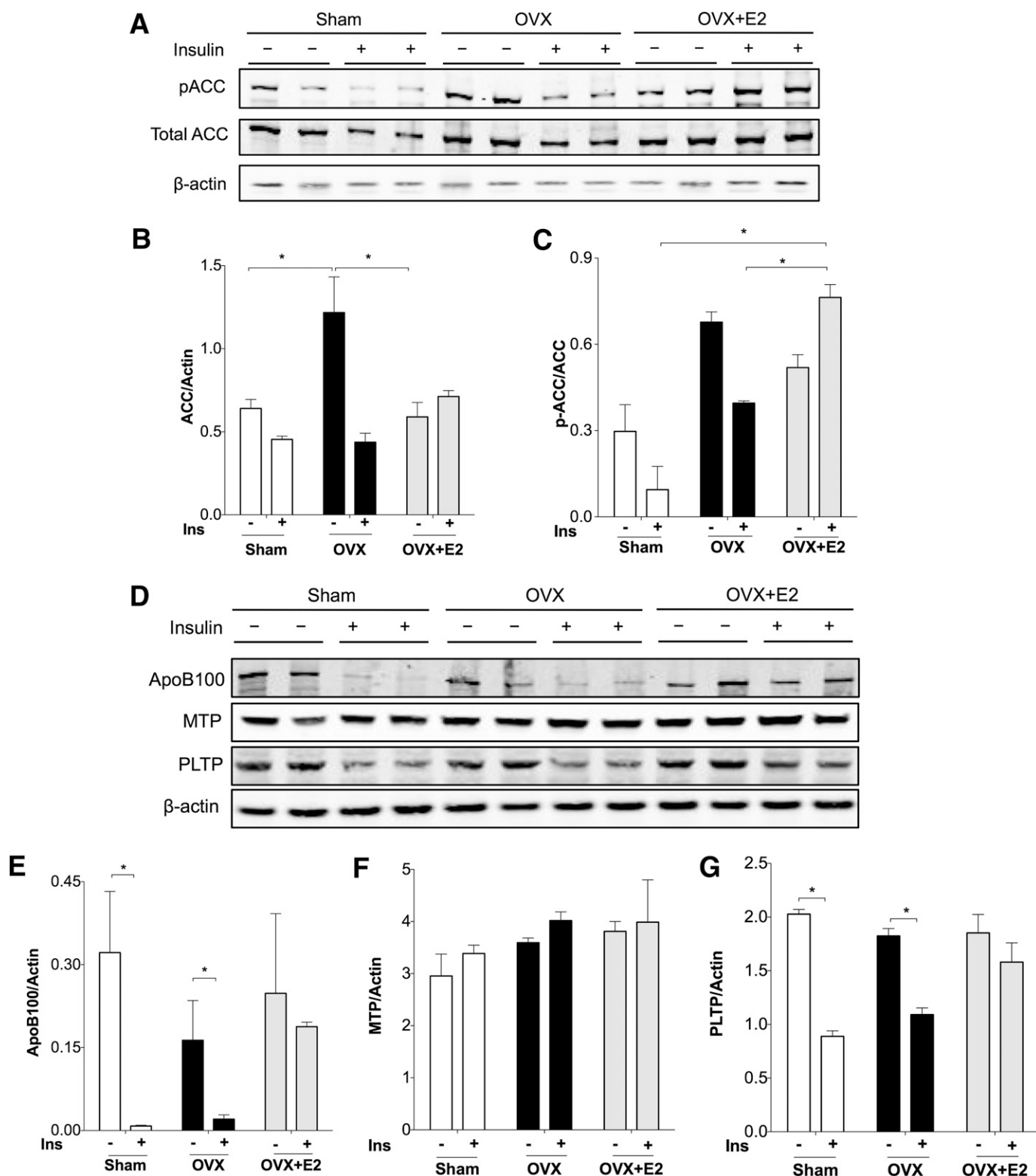


**FIG. 4.** Estrogen treatment blocks insulin (Ins)-mediated dephosphorylation of ACC and insulin reduction of apoB100 in the liver. Livers from mice in a cohort that was fasted but not clamped (–) and after hyperinsulinemic clamp study (+) were used for protein extraction and Western blotting. **A:** pACC and total ACC. Expression of actin and Panseu S staining were used as loading controls. ACC expression and the ratio of pACC to ACC were quantified in **B** and **C**. **D:** Western blot for liver apoB100, MTP, and PLTP. Expression of apoB100 (**E**), MTP (**F**), and PLTP (**G**) was quantified as well. \* $P < 0.05$ . Differences (+ or – insulin) were defined by Student *t* test. Differences between groups were determined by ANOVA followed by Tukey post hoc tests.

of whole-body versus hepatic estrogen signaling toward the improvements in insulin resistance and dyslipidemia seen with estrogen treatment after OVX. In LKO mice, liver ER $\alpha$  expression was reduced >90% from whole-liver extracts but unchanged in muscle or adipose tissue (Fig. 5A). The LKO female mice had body weight, adiposity, fasting triglyceride, and fasting glucose similar to those of their littermates on a chow diet (Supplementary Table 1).

As was observed in wild-type C57BL/6J mice, OVX was associated with increased body weight and adiposity compared with sham mice (Fig. 5B and C). Also like wild-type mice, estrogen treatment was associated with reduced body weight and reduced adiposity after OVX in LKO mice (Fig. 5B and C). These results demonstrate that the ability of estrogen treatment to protect from OVX- and diet-induced adiposity does not require intact hepatic ER $\alpha$  signaling.

In contrast to wild-type littermates, in which estrogen treatment reduced fasting triglyceride, in OVX LKO mice estrogen treatment significantly increased fasting triglyceride (Supplementary Fig. 4A). Fasting plasma cholesterol concentration was increased with OVX in both wild-type and LKO mice and reduced with estrogen treatment in both groups (Supplementary Fig. 4B). These results suggest that hepatic estrogen signaling is required for estrogen treatment to maintain low serum triglyceride after OVX. By contrast, reduction of fasting cholesterol does not appear to require liver estrogen signaling and

was more closely associated with the reduced adiposity seen in both LKO and wild-type mice with estrogen treatment.

Estrogen treatment lowered insulin levels in both LKO mice and their wild-type littermates (Supplementary Fig. 4D). Fasting glucose values were not different between groups (Supplementary Fig. 4C). Hyperinsulinemic clamp studies showed that estrogen treatment after OVX improved insulin sensitivity in wild-type littermates (Fig. 5E and Supplementary Fig. 4E). In contrast, the ability of estrogen treatment to improve insulin sensitivity after OVX was blunted in LKO mice (Fig. 5E [GIR] and Supplementary Fig. 4E [insulin sensitivity index]). Estrogen treatment did not improve insulin suppression of EndoRa in LKO mice (Fig. 5F). Additionally, estrogen treatment did not prevent insulin suppression of  $^{14}\text{C}$  tracer incorporation into serum triglyceride (Fig. 5G). These results suggest that the ability of E2 treatment to block insulin-mediated triglyceride secretion from the liver requires hepatic ER $\alpha$ . Based on this insulin suppression of triglyceride secretion, we expected to find increased liver fat in E2-treated LKO mice.

**Liver ER $\alpha$  signaling is required to prevent liver fat and diacylglycerol accumulation.** In the absence of hepatic ER $\alpha$  signaling, liver  $^{14}\text{C}$ -triglyceride deposition and triglyceride accumulation remained high with estrogen treatment in LKO mice (Fig. 6A and B), which was 2.2-fold ( $P < 0.05$ ) higher than in E2-treated wild-type controls (Fig. 3B and C). Estrogen treatment was unable to reduce

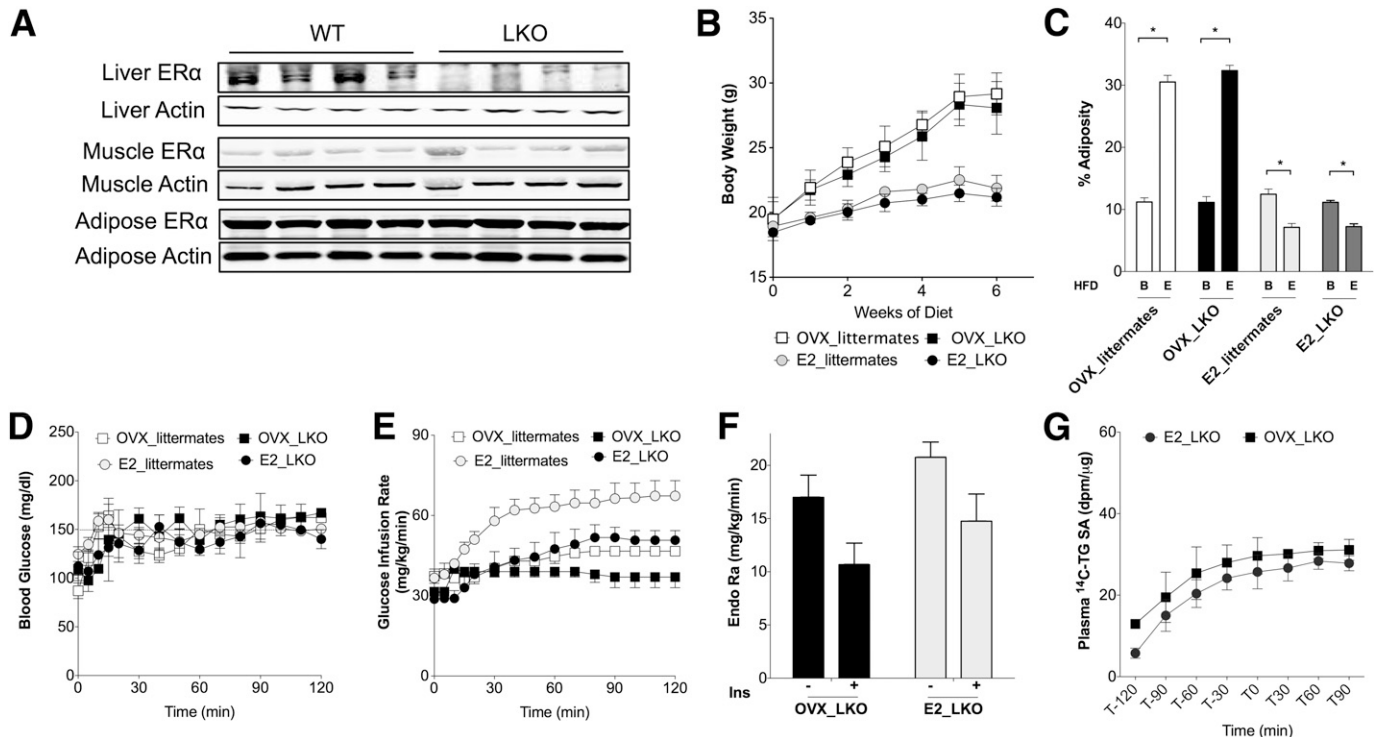


**FIG. 5.** Estrogen treatment reduces body weight but does not prevent pathway-selective insulin (Ins) resistance in LKO mice. *A:* ER $\alpha$  protein amounts were decreased specifically in liver of LKO mice but not in other tissues. *B:* Weight gain with HFD was increased after OVX and prevented with E2 treatment in LKO mice and their wild-type (WT) littermates. *C:* OVX led to increased adiposity with HFD, which was prevented with E2 treatment in LKO mice and their littermates. Letter B indicates baseline before HFD-feeding. Letter E indicates end point after HFD. *D:* Euglycemia was maintained at  $\sim 150$  mg/dL during the clamp. *E:* GIR to maintain euglycemia. *F:* Estrogen treatment did not restore the insulin suppression of EndoRa after OVX in LKO mice (–, baseline period of clamp; clamp period). *G:* Plasma  $^{14}\text{C}$ -triglyceride (TG)-specific activity (SA) was not significantly different by E2 treatment after OVX in LKO mice. \* $P < 0.05$ . Differences from baseline (B) or end point (E) were defined by Student *t* test.

total diacylglycerol and  $^{14}\text{C}$ -diacylglycerol in LKO mice (Fig. 6C and D). The ability of estrogen to block the effects of insulin with regard to ACC dephosphorylation and protein amounts of ApoB100 and PLTP was also lost in E2 LKO mice (Fig. 6E and Supplementary Fig. 5).

Thus, despite a lean body composition in E2 LKO mice, liver ER $\alpha$  signaling was required for the ability of estrogen treatment to reduce triglyceride and diacylglycerol accumulation in the liver. Taken together, these results suggest

that estrogen treatment acts through hepatic ER $\alpha$  to prevent fatty liver by suppressing triglyceride synthesis, maintaining the efficiency of triglyceride secretion from the liver (Fig. 7). In addition, hepatic ER $\alpha$  appears to be required for estrogen to improve insulin action on glucose metabolism. Thus, while E2 treatment maintained lean body composition after OVX, E2 treatment failed to reverse pathway-selective insulin resistance in the absence of hepatic ER $\alpha$ .

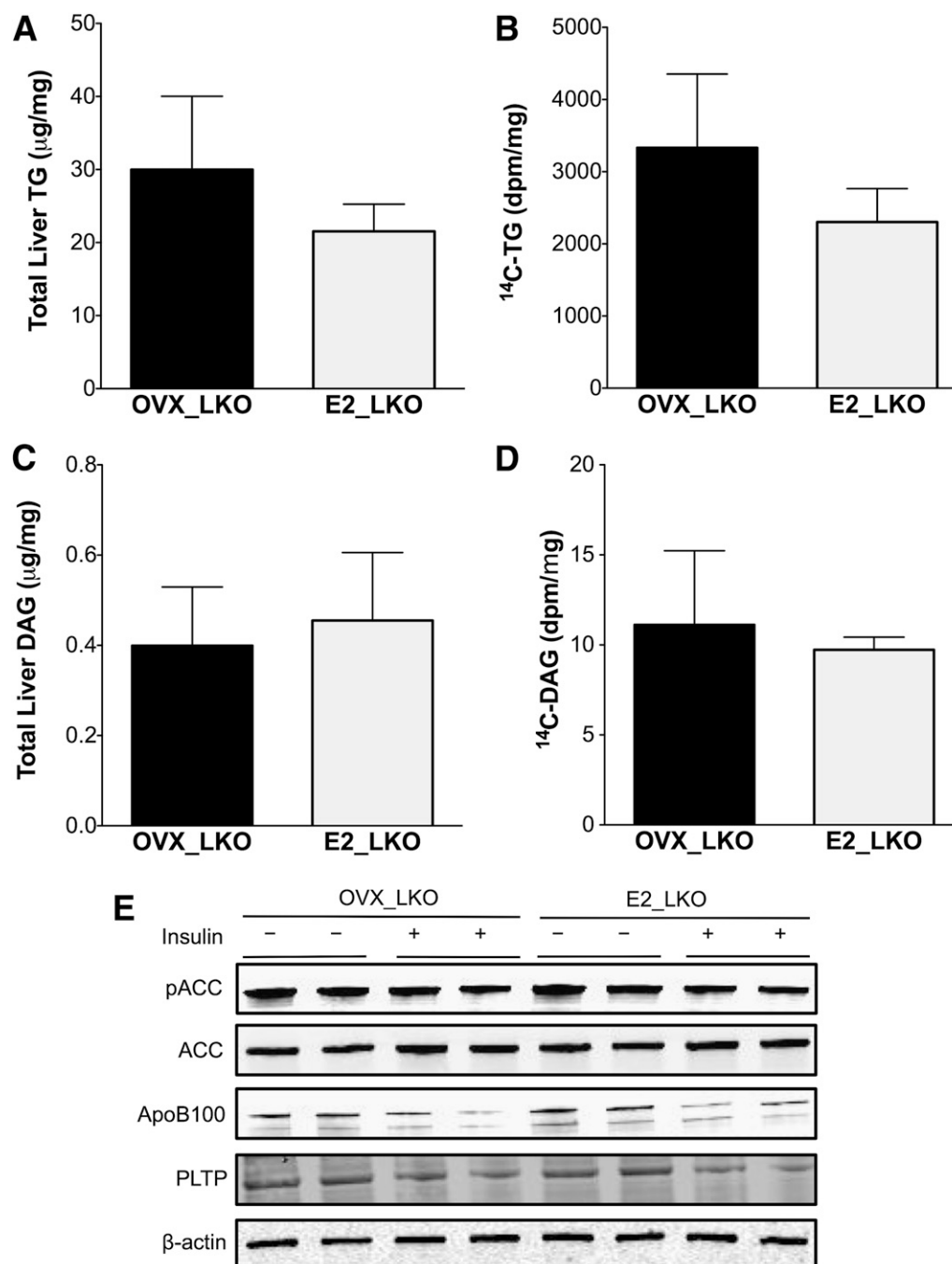


**FIG. 6.** Estrogen treatment fails to protect against fatty liver with HFD feeding in LKO mice after OVX. *A–D*: Liver lipids were extracted with the Folch method, and neutral lipids were separated by TLC as described in RESEARCH DESIGN AND METHODS. Triglyceride (TG) (*A*) and diacylglycerol (DAG) (*C*) were quantified using an enzymatic assay;  $^{14}\text{C}$ -triglyceride (*B*) and  $^{14}\text{C}$ -diacylglycerol (*D*) were quantified by scintillation counting. *E*: Livers from mice in a cohort that was fasted but not clamped (–) and after hyperinsulinemic clamp study (+) were used for protein extraction and Western blotting for pACC, total ACC, apoB100, MTP, and PLTP. Expression of actin and Panseau S staining were used as loading controls.



## DISCUSSION

Overnutrition results in pathway-selective insulin resistance, where insulin signaling is impaired with regard to glucose metabolism, yet intact with regard to fatty acid and liver triglyceride storage. We designed *in vivo* studies to simultaneously study both aspects of this biology (Fig. 7). We found HFD feeding after OVX produced such pathway-selective insulin resistance where insulin failed to suppress hepatic glucose production, yet insulin was able to reduce hepatic apoB content, maintain ACC activity, and suppress tracer incorporation into serum triglyceride. This predisposed mice to hepatic triglyceride and diacylglycerol accumulation. Estrogen treatment at the time of surgical menopause was associated with improvements in pathway-selective insulin resistance. Estrogen treatment restrained liver triglyceride deposition, prevented insulin signaling to apoB, and maintained triglyceride export from the liver. This was associated with a reduction in liver triglyceride and diacylglycerol content with HFD feeding. Reciprocally, estrogen treatment augmented the ability of insulin to regulate hepatic and peripheral glucose metabolism. Thus, estrogen treatment improved some aspects of pathway-selective insulin resistance in the liver associated with HFD feeding.

In these studies, we also defined tissue-specific roles of estrogen treatment in the setting of HFD feeding after OVX. Estrogen treatment with OVX prevented weight gain and increased adiposity with HFD feeding. This effect of estrogen treatment was seen both in wild-type mice and in LKO mice, indicating that hepatic estrogen is dispensable for body weight regulation with estrogen treatment. These findings are consistent with known effects of estrogen to reduce food intake and adiposity in the central nervous system and promote fatty acid oxidation in peripheral tissues (34,36,37). Despite lean body composition, however, estrogen-treated LKO mice had fatty liver, and estrogen treatment resulted in only modest improvement in whole-body insulin sensitivity compared with OVX LKO mice. Without hepatic estrogen signaling, there was also severe hepatic insulin resistance indicated by impaired insulin suppression of hepatic glucose production, even in lean estrogen-treated mice after OVX (Fig. 5F). Thus, hepatic estrogen signaling appears to be important for the metabolic effects of estrogen treatment with regard to

preventing fatty liver and maintaining glucose homeostasis. These results help dissociate estrogen's effects on body weight from estrogen regulation of insulin sensitivity.

We found that estrogen treatment reduces fatty liver by disrupting insulin's effects to promote liver fat storage on several levels. The drug tamoxifen, an estrogen antagonist, increases hepatic steatosis in some breast cancer patients (38). Global loss of estrogen signaling also increases liver fat in several models, including humans with ER $\alpha$  mutations, rodents after OVX, mice with global ER $\alpha$  knockout, and mice lacking aromatase (19,39,40). Here, we report an underlying mechanism by which estrogen signaling may decrease liver fat (Fig. 7). In our studies, estrogen treatment after OVX reduced liver fat accretion by 1) limiting fat synthesis indicated by  $^{14}\text{C}$  deposition into liver triglyceride and diacylglycerol, 2) blocking insulin signaling to apoB, ACC, and PLTP, and 3) maintaining the efficiency of triglyceride export from the liver in the setting of hyperinsulinemia, indicated by preserved tracer incorporation into serum triglyceride and a failure of insulin to reduce hepatic apoB. The net effect was reduced liver triglyceride and diacylglycerol compared with OVX mice. This decrease in liver triglyceride and diacylglycerol may have contributed to the improved ability of insulin to suppress hepatic glucose production and improve insulin sensitivity.

The tissue-specific effects of estrogen treatment seen in these results may have implications for human diseases. The phenotype of E2 LKO mice with HFD feeding mimics the insulin resistance, dyslipidemia, and hepatic steatosis associated with lean body composition in patients with lipodystrophy (41). The tissue-specific estrogen/ER $\alpha$  signaling seen in our model of estrogen treatment might also be helpful for understanding mechanisms for the negative effects of late estrogen treatment postmenopause with regard to cardiovascular disease. Estrogen treatment when added after insulin resistance is established in peripheral tissues may make dyslipidemia worse by promoting VLDL flux that cannot be matched with efficient VLDL clearance.

For women before menopause, sex-phenotype differences confer cardiovascular protection compared with men, which may relate to improvements in metabolic complications of obesity (13,42–45). The goal of postmenopausal hormone replacement in clinical use has been to recapitulate the protective effects of the premenopausal state; however, large-scale trials have failed to show a substantial reduction in cardiovascular events (46–48). Selectively targeting liver estrogen signaling may decrease the metabolic complications of obesity and avoid some of the harmful effects of estrogen replacement in peripheral tissues such as the vascular endothelium.

## ACKNOWLEDGMENTS

This work was supported by the Department of Veterans Affairs, the American Heart Association (10GRNT3650024), the Atlantic Philanthropies, the American Diabetes Association (1-09-IG-01), the John A. Hartford Foundation, the Association of Specialty Professors, the Vanderbilt Diabetes Research and Training Center Pilot and Feasibility Program (DK20593), and the Vanderbilt Digestive Diseases Research Center Pilot and Feasibility Program (DK058404). L.Z. was supported by the Canadian Institutes of Health Research Strategic Training Program.

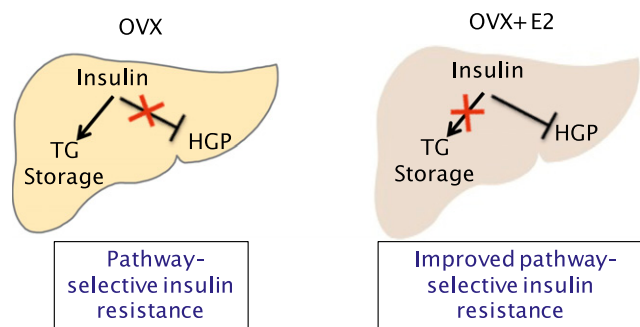


**FIG. 7.** Schematic representation of liver ER $\alpha$  signaling with regard to the regulation of liver glucose and lipid metabolism: HFD feeding after OVX resulted in pathway-selective insulin resistance where insulin failed to suppress hepatic glucose production (HGP), yet insulin was able to promote liver triglyceride (TG) storage by reducing hepatic apoB content, dephosphorylating ACC, and suppressing tracer incorporation into serum triglyceride. Estrogen treatment after OVX improved insulin suppression of hepatic glucose production and blocked insulin-mediated liver triglyceride storage.

No potential conflicts of interest relevant to this article were reported.

L.Z. researched data, wrote the manuscript, and contributed to discussion of data. W.C.B. and Q.C. researched data, reviewed and edited the manuscript, and contributed to discussion of data. A.K., P.C., and O.P.M. contributed to general discussion, reviewed and edited the manuscript, and contributed to discussion of data. J.M.S. wrote and edited the manuscript and contributed to discussion of data. J.M.S. is the guarantor of this work and, as such, had full access to all the data in the study and takes responsibility for the integrity of the data and the accuracy of the data analysis.

Parts of this study were presented in abstract form at the 71st Scientific Sessions of the American Diabetes Association, San Diego, California, 24–28 June 2011.

The authors acknowledge excellent assistance by the Vanderbilt Mouse Metabolic Phenotyping Center (DK59637) and the Vanderbilt Hormone Assay and Analytical Services Core (DK59637 and DK20593). Liver lipid was stained at the Translational Pathology Shared Resource at Vanderbilt-Ingram Cancer Center. The authors thank Dr. Vivian Siegel of Vanderbilt University School of Medicine for critical reading of the manuscript.

## REFERENCES

1. Consoli A, Nurjhan N, Reilly JJ Jr, Bier DM, Gerich JE. Mechanism of increased gluconeogenesis in noninsulin-dependent diabetes mellitus. Role of alterations in systemic, hepatic, and muscle lactate and alanine metabolism. *J Clin Invest* 1990;86:2038–2045
2. Magnusson I, Rothman DL, Katz LD, Shulman RG, Shulman GI. Increased rate of gluconeogenesis in type II diabetes mellitus. A  $^{13}\text{C}$  nuclear magnetic resonance study. *J Clin Invest* 1992;90:1323–1327
3. Han S, Liang CP, Westerterp M, et al. Hepatic insulin signaling regulates VLDL secretion and atherogenesis in mice. *J Clin Invest* 2009;119:1029–1041
4. Li S, Brown MS, Goldstein JL. Bifurcation of insulin signaling pathway in rat liver: mTORC1 required for stimulation of lipogenesis, but not inhibition of gluconeogenesis. *Proc Natl Acad Sci USA* 2010;107:3441–3446
5. Semple RK, Sleight A, Murgatroyd PR, et al. Postreceptor insulin resistance contributes to human dyslipidemia and hepatic steatosis. *J Clin Invest* 2009;119:315–322
6. Fabbri E, Magkos F, Mohammed BS, et al. Intrahepatic fat, not visceral fat, is linked with metabolic complications of obesity. *Proc Natl Acad Sci USA* 2009;106:15430–15435
7. Adiels M, Borén J, Caslake MJ, et al. Overproduction of VLDL1 driven by hyperglycemia is a dominant feature of diabetic dyslipidemia. *Arterioscler Thromb Vasc Biol* 2005;25:1697–1703
8. Lewis GF, Uffelman KD, Szeto LW, Weller B, Steiner G. Interaction between free fatty acids and insulin in the acute control of very low density lipoprotein production in humans. *J Clin Invest* 1995;95:158–166
9. Sørensen LP, Andersen IR, Søndergaard E, et al. Basal and insulin mediated VLDL-triglyceride kinetics in type 2 diabetic men. *Diabetes* 2011;60:88–96
10. Lemieux S, Prud'homme D, Bouchard C, Tremblay A, Després JP. Sex differences in the relation of visceral adipose tissue accumulation to total body fatness. *Am J Clin Nutr* 1993;58:463–467
11. Riant E, Waget A, Cogo H, Arnal JF, Burcelin R, Gourdy P. Estrogens protect against high-fat diet-induced insulin resistance and glucose intolerance in mice. *Endocrinology* 2009;150:2109–2117
12. Magkos F, Patterson BW, Mohammed BS, Klein S, Mittendorfer B. Women produce fewer but triglyceride-rich very low-density lipoproteins than men. *J Clin Endocrinol Metab* 2007;92:1311–1318
13. Mittendorfer B, Patterson BW, Klein S. Effect of sex and obesity on basal VLDL-triacylglycerol kinetics. *Am J Clin Nutr* 2003;77:573–579
14. Mittendorfer B, Patterson BW, Klein S, Sidossis LS. VLDL-triglyceride kinetics during hyperglycemia-hyperinsulinemia: effects of sex and obesity. *Am J Physiol Endocrinol Metab* 2003;284:E708–E715
15. Davis RA. Evolution of processes and regulators of lipoprotein synthesis: from birds to mammals. *J Nutr* 1997;127(Suppl.):795S–800S
16. Della Torre S, Rando G, Meda C, et al. Amino acid-dependent activation of liver estrogen receptor  $\alpha$  integrates metabolic and reproductive functions via IGF-1. *Cell Metab* 2011;13:205–214
17. Park CJ, Zhao Z, Glidewell-Kenney C, et al. Genetic rescue of nonclassical ER $\alpha$  signaling normalizes energy balance in obese ER $\alpha$ -null mutant mice. *J Clin Invest* 2011;121:604–612
18. Ohlsson C, Hellberg N, Parini P, et al. Obesity and disturbed lipoprotein profile in estrogen receptor- $\alpha$ -deficient male mice. *Biochem Biophys Res Commun* 2000;278:640–645
19. Ribas V, Nguyen MT, Henstridge DC, et al. Impaired oxidative metabolism and inflammation are associated with insulin resistance in ER $\alpha$ -deficient mice. *Am J Physiol Endocrinol Metab* 2010;298:E304–E319
20. Demissie S, Cupples LA, Shearman AM, et al. Estrogen receptor- $\alpha$  variants are associated with lipoprotein size distribution and particle levels in women: the Framingham Heart Study. *Atherosclerosis* 2006;185:210–218
21. Tian JP, Delghingaro-Augusto V, Le May C, et al. Estrogen receptor activation reduces lipid synthesis in pancreatic islets and prevents  $\beta$  cell failure in rodent models of type 2 diabetes. *J Clin Invest* 2011;121:3331–3342
22. Dupont S, Krust A, Gansmuller A, Dierich A, Chambon P, Mark M. Effect of single and compound knockouts of estrogen receptors  $\alpha$  (ER $\alpha$ ) and  $\beta$  (ER $\beta$ ) on mouse reproductive phenotypes. *Development* 2000;127:4277–4291
23. Gieske MC, Kim HJ, Legan SJ, et al. Pituitary gonadotroph estrogen receptor- $\alpha$  is necessary for fertility in females. *Endocrinology* 2008;149:20–27
24. Ayala JE, Samuel VT, Morton GJ, et al.; NIH Mouse Metabolic Phenotyping Center Consortium. Standard operating procedures for describing and performing metabolic tests of glucose homeostasis in mice. *Dis Model Mech* 2010;3:525–534
25. Steele R, Wall JS, De Bodo RC, Altszuler N. Measurement of size and turnover rate of body glucose pool by the isotope dilution method. *Am J Physiol* 1956;187:15–24
26. Ayala JE, Bracy DP, Julien BM, Rottman JN, Fueger PT, Wasserman DH. Chronic treatment with sildenafil improves energy balance and insulin action in high fat-fed conscious mice. *Diabetes* 2007;56:1025–1033
27. Zhu L, Johnson C, Bakovic M. Stimulation of the human CTP:phosphoethanolamine cytidyltransferase gene by early growth response protein 1. *J Lipid Res* 2008;49:2197–2211
28. Wu K, Cappel D, Martinez M, Stafford JM. Impaired-inactivation of FoxO1 contributes to glucose-mediated increases in serum very low-density lipoprotein. *Endocrinology* 2010;151:3566–3576
29. Swift LL, Kakkad B, Boone C, et al. Microsomal triglyceride transfer protein expression in adipocytes: a new component in fat metabolism. *FEBS Lett* 2005;579:3183–3189
30. Neschen S, Morino K, Hammond LE, et al. Prevention of hepatic steatosis and hepatic insulin resistance in mitochondrial acyl-CoA: glycerol-sn-3-phosphate acyltransferase 1 knockout mice. *Cell Metab* 2005;2:55–65
31. Mao J, DeMayo FJ, Li H, et al. Liver-specific deletion of acetyl-CoA carboxylase 1 reduces hepatic triglyceride accumulation without affecting glucose homeostasis. *Proc Natl Acad Sci USA* 2006;103:8552–8557
32. Choi SH, Ginsberg HN. Increased very low density lipoprotein (VLDL) secretion, hepatic steatosis, and insulin resistance. *Trends Endocrinol Metab* 2011;22:353–363
33. Tamura S, Shimomura I. Contribution of adipose tissue and de novo lipogenesis to nonalcoholic fatty liver disease. *J Clin Invest* 2005;115:1139–1142
34. D'Eon TM, Souza SC, Aronovitz M, Obin MS, Fried SK, Greenberg AS. Estrogen regulation of adiposity and fuel partitioning. Evidence of genomic and non-genomic regulation of lipogenic and oxidative pathways. *J Biol Chem* 2005;280:35983–35991
35. Lie J, de Crom R, van Gent T, et al. Elevation of plasma phospholipid transfer protein in transgenic mice increases VLDL secretion. *J Lipid Res* 2002;43:1875–1880
36. Musatov S, Chen W, Pfaff DW, et al. Silencing of estrogen receptor  $\alpha$  in the ventromedial nucleus of hypothalamus leads to metabolic syndrome. *Proc Natl Acad Sci USA* 2007;104:2501–2506
37. Perreault L, Bergman BC, Hunerdosse DM, Eckel RH. Altered intramuscular lipid metabolism relates to diminished insulin action in men, but not women, in progression to diabetes. *Obesity (Silver Spring)* 2010;18:2093–2100
38. Oien KA, Moffat D, Curry GW, et al. Cirrhosis with steatohepatitis after adjuvant tamoxifen. *Lancet* 1999;353:36–37
39. Bryzgalova G, Gao H, Ahren B, et al. Evidence that oestrogen receptor- $\alpha$  plays an important role in the regulation of glucose homeostasis in mice: insulin sensitivity in the liver. *Diabetologia* 2006;49:588–597

40. Jones ME, Thorburn AW, Britt KL, et al. Aromatase-deficient (ArKO) mice have a phenotype of increased adiposity. *Proc Natl Acad Sci USA* 2000;97:12735–12740
41. Huang-Doran I, Sleigh A, Rochford JJ, O'Rahilly S, Savage DB. Lipodystrophy: metabolic insights from a rare disorder. *J Endocrinol* 2010;207:245–255
42. Roger VL, Go AS, Lloyd-Jones DM, et al.; American Heart Association Statistics Committee and Stroke Statistics Subcommittee. Heart disease and stroke statistics—2011 update: a report from the American Heart Association. *Circulation* 2011;123:e18–e209
43. Keil JE, Sutherland SE, Knapp RG, Lackland DT, Gazes PC, Tyroler HA. Mortality rates and risk factors for coronary disease in black as compared with white men and women. *N Engl J Med* 1993;329:73–78
44. Fontaine KR, Redden DT, Wang C, Westfall AO, Allison DB. Years of life lost due to obesity. *JAMA* 2003;289:187–193
45. Martinez MN, Emfinger CH, Overton MH, et al. Obesity and altered glucose metabolism impact HDL composition in CETP transgenic mice: a role for ovarian hormones. *J Lipid Res* 2012;53:379–389
46. Rossouw JE, Prentice RL, Manson JE, et al. Postmenopausal hormone therapy and risk of cardiovascular disease by age and years since menopause. *JAMA* 2007;297:1465–1477
47. Manson JE, Hsia J, Johnson KC, et al.; Women's Health Initiative Investigators. Estrogen plus progestin and the risk of coronary heart disease. *N Engl J Med* 2003;349:523–534
48. Rossouw JE, Anderson GL, Prentice RL, et al.; Writing Group for the Women's Health Initiative Investigators. Risks and benefits of estrogen plus progestin in healthy postmenopausal women: principal results from the Women's Health Initiative randomized controlled trial. *JAMA* 2002;288:321–333